

## Azimuthal anisotropy analysis from P-wave seismic traveltimes

*Kenneth L. Craft \*, Subhashis Mallick, Laurent J. Meister, and Richard Van Dok, Western Geophysical*

### SUMMARY

The oil and gas industry recently has shown a strong interest in the existence and detection of natural fracture systems. These fracture systems can produce viable porosity and permeability in reservoir rock matrices that otherwise would not be of economic interest.

When fracture systems consist of azimuthally aligned, vertically oriented cracks, azimuthal variations in amplitude variation with offset can be observed in multi-azimuth P-wave surface seismic data. (Mallick, et al, 1996) Additionally, traveltimes anomalies can be observed in conventional velocity analyses performed on azimuthally segregated gathers. This paper will describe a method of measuring and quantifying the traveltimes anomalies and representing the resulting information in a fashion which can be integrated with other geologic and geophysical information.

### INTRODUCTION

Detection of natural fracture systems using surface seismic measurements has gained considerable attention from the oil and gas industry over the past few years. With the advent of horizontal drilling technology, fracture detection capabilities from surface seismic have gone from desirable to essential.

Existence of oriented fracture systems induce azimuthal anisotropy (AA) in rock matrices that would otherwise be azimuthally isotropic. Propagation of shear waves in AA media is sensitive to its direction of propagation with respect to the orientation of fractures. Consequently, multi-component shear wave seismic data have traditionally been used for fracture detection. Acquisition and processing of multi-component data is expensive. In addition, signal-to-noise (S/N) ratios in multi-component shear wave data is often very low. Considering the facts that single-component data are significantly less costly to acquire and process than shear data, and that S/N ratios of P-wave data are generally higher, Mallick et. al. (1996) have demonstrated that reflection amplitudes of multi-azimuth P-wave data can be used to find fracture orientation and a qualitative measure of fracture density.

Although amplitude analysis has worked on some real data, processing requirements for preserving relative amplitudes in multi-azimuth data are rather stringent. In addition, near surface heterogeneity and subsurface lateral inhomogeneity can severely affect data amplitudes. Since traveltimes are not as sensitive to these inhomogeneities, they were used in the present investigation to develop a more robust azimuthal P-wave fracture detection method.

### DATA ACQUISITION ISSUES - GEOMETRY AND GEOLOGY

The azimuthal P-wave seismic traveltimes method analyzes gathers at a variety of source-receiver azimuths at a given location to search for azimuthal velocity variations. This implies that data must contain a sufficient range of offsets to allow accurate normal moveout analyses in several directions. Typically, angles of incidence of 20 to 30 degrees are required to produce analysis sets capable of extremely accurate velocity interpretations. Obviously, the deeper the analysis target, the larger the spread must be to achieve offsets corresponding to such angles. Simple 2D approaches can be used to produce reasonable geometry for the velocity measurements, but are prone to inconsistencies in long wavelength statics solutions. Wide azimuth 3D surveys are therefore preferable. Figure 1 shows the offset-azimuth distribution produced with all possible combinations of inline and crossline offsets ranging from -2975 to +2975 meters by 50 meters.

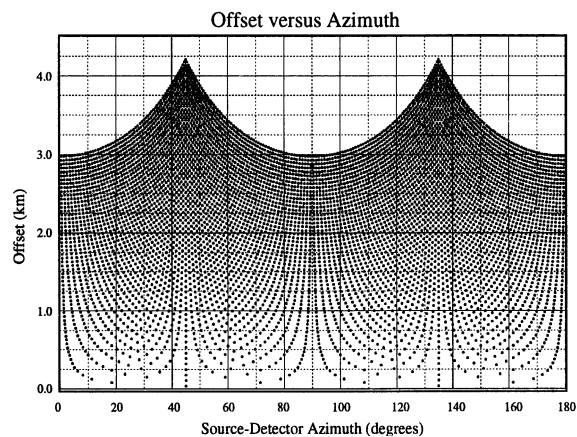


Figure 1. Offset vs. azimuth plot for an ideal geometry

Even when allowing for the removal of reciprocal raypaths, this sampling requires 7200 traces, and after elimination of offsets greater than 3000 meters, 5700 traces remain. Typically, such an offset-azimuth distribution is not to be found in a single CMP gather. In a simple survey with orthogonal shot and receiver lines, the fundamental pattern of offset and azimuth repeats twice in each rectangle of one shot line by one receiver line. The coarser these line spacings, the larger the "superbin" required for complete sampling of offset and azimuth. The size of this bin, in conjunction with the dip and variability of reflectivity of events of interest, can complicate the analysis. Fortunately, many reservoirs with natural fractures are relatively flat.

## Anisotropy from P-wave traveltimes

Typically, onshore surveys, with their relatively expensive shots, require very large numbers of receivers to achieve acceptable geometries. Marine bottom cable operations, with inexpensive airgun shots and relatively intensive receiver placement efforts, require very large numbers of shots. Marine streamer operations are virtually unable to produce azimuthal sampling adequate for P-wave anisotropy analysis.

### DATA PROCESSING - MAINTAINING DIFFERENTIAL TRAVELTIMES

Picking of traveltimes at its simplest consists of hyperbolic normal moveout velocity analyses for stacking velocity determination. As perturbations of traveltime from a hyperbolic function of offset can seriously impair the integrity of stacking velocity, it is important to resolve near surface statics for all wavelengths. Wavelet processing should be used to produce a consistent wavelet. Random and coherent noise removal is also instrumental in allowing reasonable interpretation of NMO velocity. Unlike amplitude analysis, traveltimes are distorted by very few seismic data processes when these processes are used in a consistent fashion with reasonable statistical support.

### THE METHOD

It has long been noted that fracture systems produce an azimuthal anisotropy in seismic velocity. (Crampin, et al., 1980) A single system of vertically oriented, parallel cracks will produce faster measured P-wave velocity in the direction of the cracks than in the direction perpendicular to the cracks. Since seismic velocity analyses depend on the traveltime differentials as a function of offset due to the significant horizontal component of wave travel, they are particularly sensitive to this azimuthal variation in rock velocity. Figure 2 shows the azimuthal variation in traveltime evident in 18 azimuth gathers constructed from a superbin taken from a wide azimuth 3D survey. All gathers have been corrected with a common normal moveout velocity function.

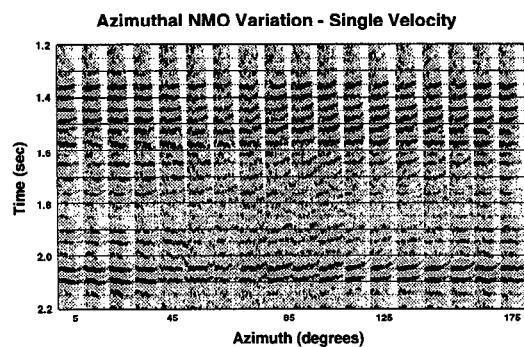


Figure 2. Binned azimuth gathers each 10 degrees moved out with a single time variant velocity function.

Figure 3 shows three common offset gathers selected from the traces in Figure 2. The traveltimes to each reflector in this view are clearly sinusoidal. Figure 4 shows measured stacking velocity contours as a function of time and azimuth. Using 180 degree periodicity only, corresponding to a single system of cracks or a narrow range of crack azimuths (for details see

Crampin, et al., 1980), the interval velocity in each layer can be represented in the following form:

$$V(\alpha) = A + B * \text{Cos} ( 2*(\phi - \alpha) )$$

where A - is mean interval velocity,  
B - is modulation of interval velocity  
 $\phi$  - is the azimuth of peak interval velocity  
and  $\alpha$  - is the angle of observation for each velocity analysis.

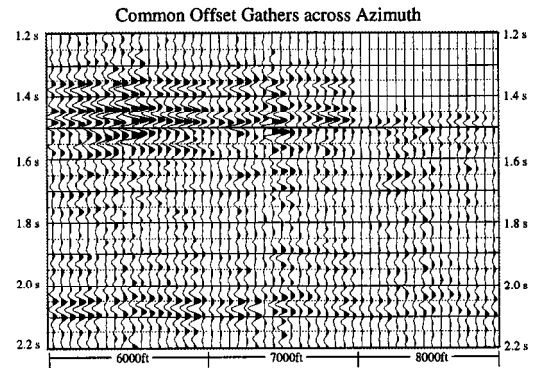


Figure 3. Common offset gathers ranging across azimuth.

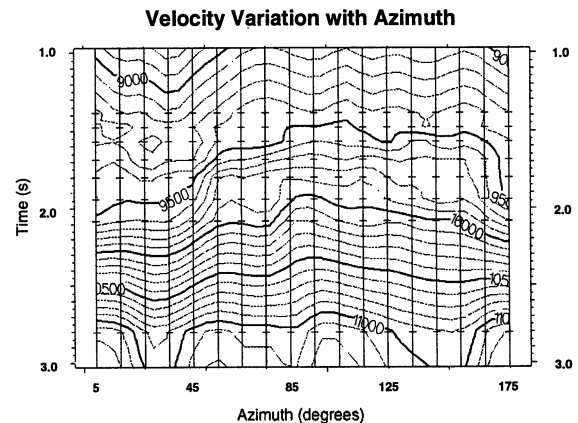


Figure 4. Velocity contours showing the variation of stacking velocity with time and azimuth. Closely spaced tics correspond to detailed interpretation in the primary zone of interest.

We can form a least square error fit as a function of azimuth to interval velocity computed from the interpreted stacking-velocity functions. Figure 5 shows such a fit on a selected interval. Notice that the RMS error of the fit is rather large (one half) relative to the modulation of interval velocity. Clearly, nominal instability of interval velocities computed in this way can vary wildly with small errors in representation of the stacking velocity.

However, stacking velocity measurements are generally quite stable and, while fits of stacking velocity at the top and bottom of this layer yield much smaller moduli than from interval velocity, the RMS error of each fit is smaller compared to its modulus (about 28 percent). It is reasonable

## Anisotropy from P-wave traveltimes

to perform the same kind of fit on RMS as interval velocity since RMS velocity is simply an integrated form of interval velocity and all components of the fit are differentiable and integrable. Figure 6 shows a fit to interval velocity measurements computed from the fitted RMS functions from the top and bottom of the layer. Note that there is almost no error and that the fit parameters, A, B, and  $\phi$  are almost exact matches of those from the raw interval velocity. It is important to note that the orientation and modulus of interval velocity are encoded in the changes as a function of time of the orientation and modulus of the stacking velocity.

A = 10990.46, B = 1045.44, Phi = 102.30 deg., RmsErr = 522.15

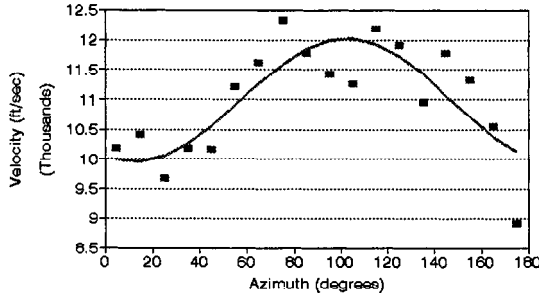


Figure 5. Fit of raw Dix interval velocity measured at 18 azimuths.

A = 11002.25, B = 1034.53, Phi = 102.43 deg., RmsErr = 10.92

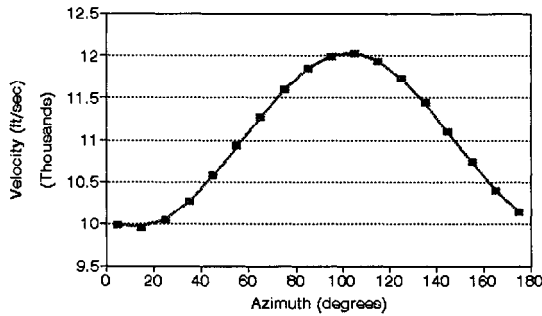


Figure 6. Fit to Dix interval velocity computed from fitted (azimuthally smoothed) stacking velocities.

### CONTINUOUS TIME ANALYSIS

At this point, we have shown a method for computing and expressing anisotropy in the form of a measurement of A, B, and  $\phi$  for one layer at one location. A simple extension of the above method will allow us to produce anisotropy estimates continuously in time at a given location. This is done by resampling each interpreted velocity function to a consistent time interval, such as 4 msec. Then, for each time sample, a fit is performed to the stacking velocity functions, producing time traces of A, B,  $\phi$ , and RMS error. The input velocity traces are then replaced with fitted values computed at the original observation azimuths. Figure 7 is a contour of the fitted stacking velocity. Note that the trend of the contour is not significantly different than that shown in Figure 4.

Constant time Dix interval velocity is then computed for each fitted function. The fixed interval used is selected to be slightly shorter than the minimum temporal resolution of the interpreted velocity functions. The interval velocity values are placed in

traces at the time in the center of the computation interval. The fit is then performed on each sample of the interval velocity as a function of azimuth, yielding interval A, B,  $\phi$ , and RMS error. Figure 8 is a representation of this type of analysis produced from the example gather using a 60 msec fixed interval. The interval anisotropy orientation and magnitude results correlate very well with the "LS fractogram", (Mallick, et al., 1996) study performed at the same location and the results of a three component VSP study made at a nearby well.

### Velocity after Curve Fit

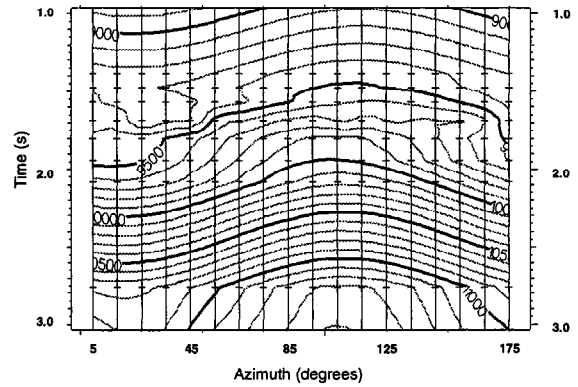


Figure 7. Velocity contours after azimuthal fit. Note that changes are minimal relative to Figure 4.

### Interval Velocity Anisotropy Plot

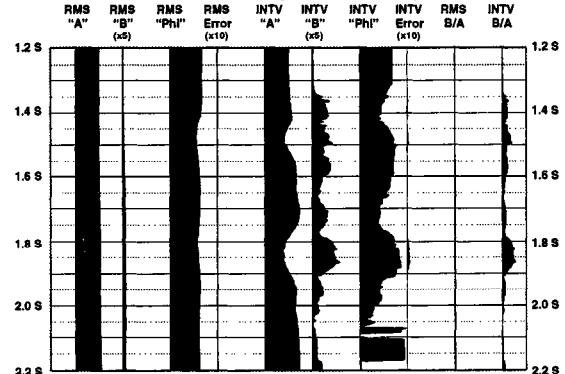


Figure 8. Traveltime "Fractogram" plot of stacking and interval velocity. Note that "B" and RMS error values are exaggerated by factors of 5 and 10, respectively, relative to "A" plots. The Phi traces are plotted such that one trace space = 180 degrees.

### VOLUME ANALYSIS

Provided that velocity analyses can be produced with adequate spatial and azimuthal sampling, interval velocity anisotropy attributes can be computed for an entire interior volume of a multi-azimuth survey. Such an exercise was performed on a small 3D survey acquired over an active gas play in the Rulison Field, Piceance Basin, Colorado (Decker et al., 1997).

The data for the entire survey were divided into four azimuth volumes of 45 degrees width, centered on 15, 60, 105 and 150 degrees, respectively. At selected locations, velocity analyses were produced and interpreted using data

# Anisotropy from P-wave traveltimes

from each of the volumes independently. The velocity volumes were then interpolated to each CMP position in the survey and azimuthal anisotropy analyses run at each location. The resulting volumes of azimuthally averaged interval velocity ("A"), azimuthal modulus of interval velocity ("B"), and orientation of maximum interval velocity (" $\phi$ ") were then analyzed on an interactive 3D interpretation system along with the 3D stack volume.

Figure 9 shows a computed apparent percentage of anisotropy map for a 200 msec thick volume located immediately above the marker generally considered to be the bottom of a gas reservoir. This is produced by dividing the "B" volume by the sum of the "A" and "B" volumes and multiplying the result by 200. While this quantity may not exactly represent the actual magnitude of the anisotropy, it should yield a positive correlation to fracture density.

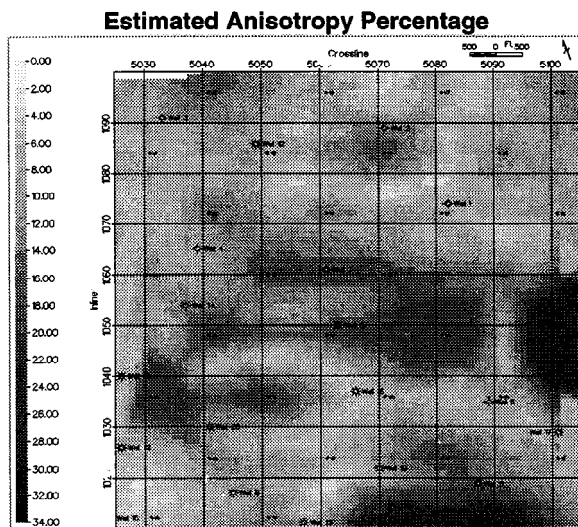


Figure 9. Observed Anisotropy Percentage computed over a 200 msec window above an interpreted marker.

Figure 10 shows the orientation of maximum interval velocity or  $\phi$ , computed on the same interval. The orientation and magnitude of anisotropy can be compared to borehole measurements and interpretations of faults and other mechanisms that generated the stresses that would produce fractures. Although direct correlation of these maps to well production and estimated recoverable reserves is incomplete, cautious optimism has been expressed by the scientists involved in the data evaluation that direct correlation will be possible with improved sampling and a targeted interpretation approach.

## ADDITIONAL WORK

The methods described in this paper can be improved and their applicability extended by developing additional tools for removing the effects of structural variation and overburden complexity from the analyses. Research in these areas is ongoing.

## CONCLUSIONS

Azimuthal anisotropy analysis and, consequently, fracture system detection can feasibly be performed using P-wave surface seismic traveltimes. Under conditions where adequate spatial and azimuthal sampling is available, volume analysis can be a powerful exploration tool.

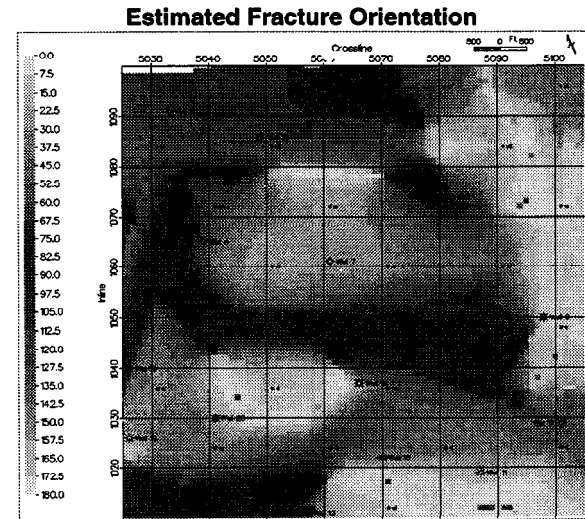


Figure 10. Observed Anisotropy Orientation from same volume and location as Figure 9.

## ACKNOWLEDGEMENTS

We would like to thank Western Geophysical for its permission to publish this work, Heloise B. Lynn for her continued support and interest, and the U.S. Dept. of Energy for its active support of innovative methods to improve industry efficiency in finding oil and gas.

## REFERENCES

- Crampin, S., McGonigle, R., and Bamford, D., 1980, Estimating crack parameters from observations of P-wave velocity anisotropy: *Geophysics*, 45,345360
- Decker, D., Lynn, H. B., Kuuskraa, V., 1997, Field Study III: Rulison Field, Piceance Basin, Colorado: Proceedings from "Seismic Detection and Analysis of Naturally Fractured Gas Reservoirs" Geophysical Applications, D.O.E. Natural Gas Conference Workshop, Houston, Texas.
- Mallick, S., Craft, K., Meister, M., and Chambers, R., 1996, Computation of principal directions of azimuthal anisotropy from P-wave seismic data: 66th Ann. Internat. Mtg. Soc. Expl. Geophys., Expanded Abstracts, 1862- 1865.